Iraqi Journal of Physics, 2019 *Vol.17, No.43, PP. 103-121*

DOI: 10.20723/ijp.17.43.103-121

Behavior of earth magnetosphere radius during strong geomagnetic storms

Mays M. Al-Gbory and Najat M. R. Al-Ubaidi

Department of Astronomy and Space, College of Science, University of Baghdad,

Baghdad, Iraq

E-mail: maisalgbory@yahoo.com

Abstract

Magnetosphere is a region of space surrounding Earth magnetic field, the formation of magnetosphere depends on many parameters such as; surface magnetic field of the planet, an ionized plasma stream (solar wind) and the ionization of the planetary upper atmosphere (ionosphere). The main objective of this research is to find the behavior of Earth's magnetosphere radius (R_{mp}) with respect to the effect of solar wind kinetic energy density (Usw), Earth's surface magnetic field (B_o), and the electron density (N_e) of Earth's ionosphere for three years 2016, 2017 and 2018. Also the study provides the effect of solar activity for the same period during strong geomagnetic storms on the behavior of R_{mp}. From results we found that there are nonlinear relations between the (R_{mp}) and the three variables (Usw), (B_o) and (N_e). In addition we found that during the strong geomagnetic storms there is a reduction in the radius of magnetosphere.

Key words

Magnetosphere, solar wind, surface magnetic field, ionosphere, and geomagnetic storms.

Article info.

Received: Sep. 2019
Accepted: Oct. 2019
Published: Dec. 2019

سلوك نصف قطر الماكنيتوسفير للأرض خلال ظروف جيومغناطيسية مختلفة

ميس محمد الجبوري و نجاة محمد رشيد العبيدي

قسم الفلك والفضاء، كلية العلوم، جامعة بغداد، بغداد، العراق

الخلاصة

الماكنيتوسفير هي المنطقة من الفضاء التي تحيط بالمجال المغناطيسي للأرض، تكوين هذه المنطقه يعتمد على عدة عوامل على سبيل المثال المجال المغناطيسي للكوكب وحزمة البلازمة المتأينة (الرياح الشمسية) والطبقة المتأينة من الغلاف الجوي العلوي للكوكب (الايونوسفير). الهدف الرئيسي من هذا البحث ينصب حول معرفة تصرف نصف قطر الماكنيتوسفير (R_{mp}) وعلاقته بتأثير الطاقه الحركية للرياح الشمسيه (U_{SW}) والمجال المغناطيسي السطحي للارض (B_o) والكثافة الالكترونية لطبقة الايونوسفير (N_e) على تكوين ماكنيتوسفير الأرض وللسنوات 2016 و2017 و2018. وأيضا تتضمن الدراسة تأثير النشاط الشمسي لنفس الفتره خلال العواصف الجيومغناطيسيه القويه على تصرف R_{mp}. من النتائج تبين ان هنالك علاقة غير خطيه بين نصف قطر الماكنيتوسفير والمعاملات (U_{sw}) و(B_o) و(N_e). كما وجدنا أنه خلال العواصف الجيومغناطيسيه القوية يحدث انكماش في نصف قطر الماكنيتوسفير.

Introduction

Formation of the Earth's magnetosphere depends on several factors, including the solar wind, Earth magnetic field and the electron density of the ionosphere. Magnetosphere is surrounding an astronomical object in which charged particles are affected by that object's magnetic field. It is created by a planet having an active interior current, in the surroundings space and close to a planetary body; the magnetic field looks like a magnetic dipole [1]. The magnetic

field lines is distorted by the current of electrically conducting plasma, such as the solar wind which is emitted from the Sun [2]. As the solar wind pressure fluctuated reduced or expanded due to situation of the solar wind activity, the magnetosphere radius or size disturbed in response, due to the balance between the pressure of the dynamic magnetic field of Earth and the dynamic pressure of the solar wind this radius can be determined [3]. When the solar wind dynamic pressure increases, the magnetopause comes closer to the Earth [4]. Earth have an active magnetosphere [5]. Many researchers studied the behavior of magnetosphere and the variation of magnetopause location, (Baraka, and Ben-Jaffel, 2007, 2011) proposed a new approach to study the sensitivity of the Earth's magnetosphere to the variability of the solar wind bulk velocity. In their study they are using a three-dimensional electromagnetic particle-in-cell code, with the microphysics interaction by simulation technique. This model developed by (Baraka, 2016) he proposed a three dimensional (3D) macro particle kinetic model (PIC) [6, 7]. Keyser et al. (2014) presents a brief overview of the magnetosphere-ionosphere system under quiet conditions, followed by a summary of the most important dynamic effects during disturbed conditions [8]. Nemecek et al. (2016) have studied the distance from Earth to the magnetosphere (magnetopause) which is varies over time due to solar activity, but the most probable upstream parameters influencing the magnetopause location are the solar wind velocity and solar ultraviolet (UV) radiation [4]. The observed magnetosphere data is analysis and compare with Shue et al. 1997 magnetosphere pause model. This analysis reveals that the magnetopause location depends on the solar activity, being more compressed during the solar maximum [9]. Ramy et al. (2016) calculated the size of the Magnetosphere during the period 1996-2011. They discovered that the magnetopause distance (D) is quantized for $D \geq 8R_E$; R_E is the Earth's radius; the magnetic levels are narrow towards the Earth but widely spaced outwards. This quantization disappears in the lower magnetosphere below $7R_E$. Once the magnetopause is compressed to $8\text{-}7R_E$ the quantization disappears and the magnetic lines of force get open allowing the solar wind to enter the inner magnetosphere and from it to the ionosphere and troposphere. They found that the mean value of magnetopause distance is about $7R_E$. Magnetopause distance differed during certain events to reach its maximum value of about $11R_E$ during 2002 and its minimum value of about $5R_E$ during 2003. The mean value of magnetopause distance is $11R_E$ for the slow solar wind, while for the fast solar wind the mean value of magnetopause distance decreased to less than $5R_E$. The size of the magnetosphere is controlled directly by the solar wind density and velocity variations [10]. Kumar et al. (2017) studied the relationship between solar wind parameters solar wind speed and interplanetary magnetic field with geomagnetic activity. The results show that there are a positive correlation between these parameters, there is a maximum correlation between the products of solar wind speed by interplanetary magnetic field with geomagnetic activity index [11]. Baker (2017) showed how high energy particles are accelerated, transported, and lost in the magnetosphere due to interplanetary shock wave interactions, coronal mass ejection impacts, and high-speed solar wind streams [12]. Reik V. Donner et al. (2018) they study the complex signatures of the

nonlinear dynamics of Magnetosphere fluctuations during non-storm and storm conditions exhibited by hourly values of the disturbance storm-time (Dst) index [13]. Khazanov et al. (2018) studied the impact of precipitating electrons and magnetosphere-ionosphere coupling processes on the ionospheric conductance [14].

The aim of this research is to study the behavior and variations of the Earth's magnetosphere radius during quiet and disturbed solar geomagnetic conditions through the Dst-index for years 2016, 2017 and 2018. Also the relation between the magnetosphere radius and the kinetic energy density of the solar wind (U_{sw}), Earth's surface magnetic field (B_o), $F_{10.7}$ index and the electron density (N_e) for Earth's ionosphere F_2 layer. The statistical correlation functions are used to find the relation between the parameters taken. Future applications of these measures for more years which include geomagnetic storms may allow us to predict the space weather condition.

Radius of magnetosphere

The distance away from Earth planet where the magnetosphere can withstand the solar wind pressure is called the "magnetopause (R_{mp})" which exists at a distance of several hundred kilometers above Earth's surface. This distance calculated by Eq. (1), where (R_e) is the radius of the Earth, (B_o) is the surface magnetic field of the Earth at the equator, (v_{sw}) is the velocity of the solar wind, (ρ_{sw}) is the mass density of the solar wind= m_p x n_{sw} (m_p is the proton density and n_{sw} is the density of solar wind near the Earth), and (μ_0) the permeability:

$$R_{mp} = R_e \left[\frac{2B_o^2}{\mu_o \rho_{sw} v_{sw}^2}\right]^{1/6} \quad (1)$$

The magnetosphere can classified according to R_{mp} values into: intrinsic magnetosphere when ($R_{mp} >> R_e$), Earth exhibits intrinsic magnetosphere. And induced magnetosphere when ($R_m << R_e$), In this type the solar wind interacts with the atmosphere or ionosphere of the planet [10].

Data selection

In this research the data were obtained from the GSFC/SPDF OMNIWeb interface, (https://omniweb.gsfc.nasa.gov/form/dx1.html) for the solar wind speed (v_{sw}) and density (n_{sw}), surface magnetic field (B_o), solar indices disturbance storm time ((Dst), sunspot number (SSN) and solar flux ($F_{10.7}$). while the data for the critical frequency f_oF_2 converted to electron density (N_e) for ionospheric F2 layer are taken from WDC for Ionosphere, Tokyo, (http://wdc.nict.go.jp/cgi-bin/ionog/man ualfv.cgi) during the years 2016-2018.

Results and discussion

Fig.1 (e, f, and g) represent the daily average solar indices Dst, SSN, and $F_{10.7}$ for the years 2016-2018 respectively, Dst reveals five events in which strong geomagnetic storms occurred (Dst > -100nT) during the period selected in this research shown in Table 1, two of them in January and October/2016, two in May and September/2017 and only one in August/2018.

Earth's magnetosphere radius (R_{mp}) is calculated by using Eq. (1), Fig.1 (a) shows this radius during the same period. There are fluctuation in the behavior of the Earth's magnetosphere radius along the years chosen, its values ranged between 7-15 R_e (R_e is the radius of Earth), their values in year 2016 are greater than values in 2017 and 2018, but the maximum value appeared in Jan. 2018. While Fig.1 (b, c, d) represented the monthly median calculations of (B_o), (U_{sw}) and (N_e) for the years 2016-2018 respectively. This figure reveals that

during the strong geomagnetic storms there are reduction in the radius of magnetosphere may be due to the ionization increases in the ionosphere during the storm time which leads to increase in the plasma conductivity, thus leading to decrease in R_{mp}, also the same happen with the magnetic field the geomagnetic storms causes disturbances in the magnetic field leading to reduction in R_{mp}. Fig.2 represents the three years 2016-2018 hourly average Earth's (R_{mp}) with (B_o, U_{sw} and N_e), show that there are nonlinear relation between the magnetosphere radius and the other parameters along each hour from the years chosen in this research. For more detail relation the ratio between R_{mp} and each parameter (B_o, U_{mp} and N_e) are taken separately with the monthly median along the three years chosen, Figs.3-11 show that respectively. From the polynomial fitting we can get the variation function equations for the magnetosphere radius with each parameter which is illustrated on the figures and their coefficients given in Tables 2-10 for each year and for each parameter respectively. These functions are very important for forecasting space weather condition if further studies are taken for more years which include geomagnetic storms.

Conclusion

From results it seems that the radius of Earth's magnetosphere varies nonlinearly with all parameters (B_o), (U_{sw}) and (N_e) taken in this research for the years 2016- 2018. During strong storms, there are reduction the radius of the magnetosphere that may be due to increase in the ionization in the ionosphere leading to increase in the conductivity of the plasma. This enhancement different from one geomagnetic storm to the other.

Acknowledgment

This work relates to University of Baghdad/ College of Science/ Department of Astronomy and Space. The data are provided from the SPDF OMNI Web database, OMNI, also the data of critical frequency (F2 layer electron density) provided from NICT Ionospheric Sounding Data, Japan, for whom I would like to introduce my utmost appreciation and thanks for their cooperation.

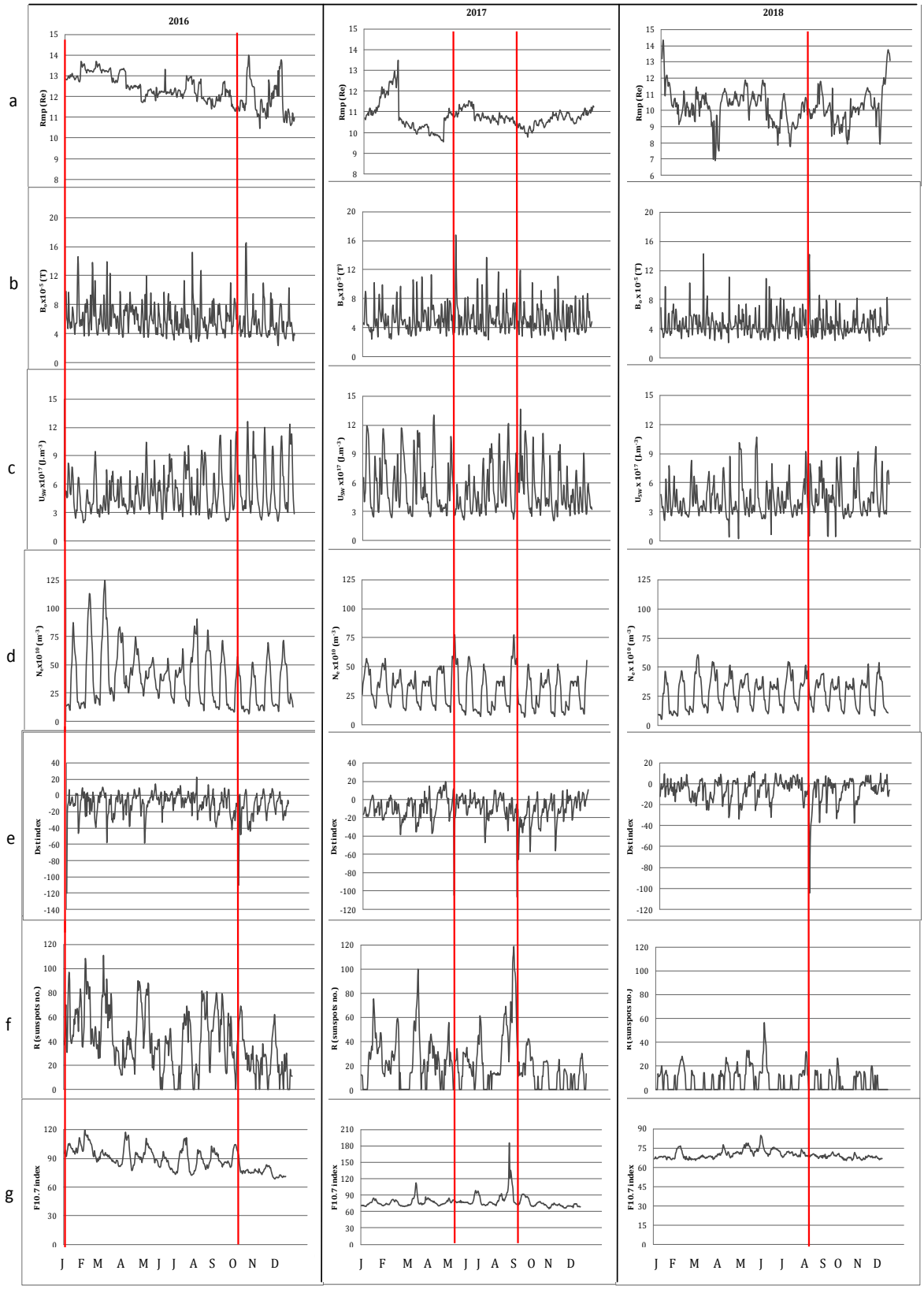

Fig. 1: Daily average of: a) R_{mp}*R_e km , b) B_ox10^{-5} T, c) U_{SW}x10^{17} j/m^3, d) N_ex10^{10} m^{-3}, e) Dst index nT, f) Sunnspots no. (R) and g) F10.7 index for years 2016-2018.

Table 1: Strong geomagnetic storms occurred through the years 2016-2018.

event no.	day	month	year	time of storm (hour)	storm type
1	1	1	2016	0-1	Strong
2	10	10	2016	23	Strong
3	28	5	2017	5-8	Strong
4	7	9	2017	13-22	Strong
5	26	8	2018	3-12	Strong

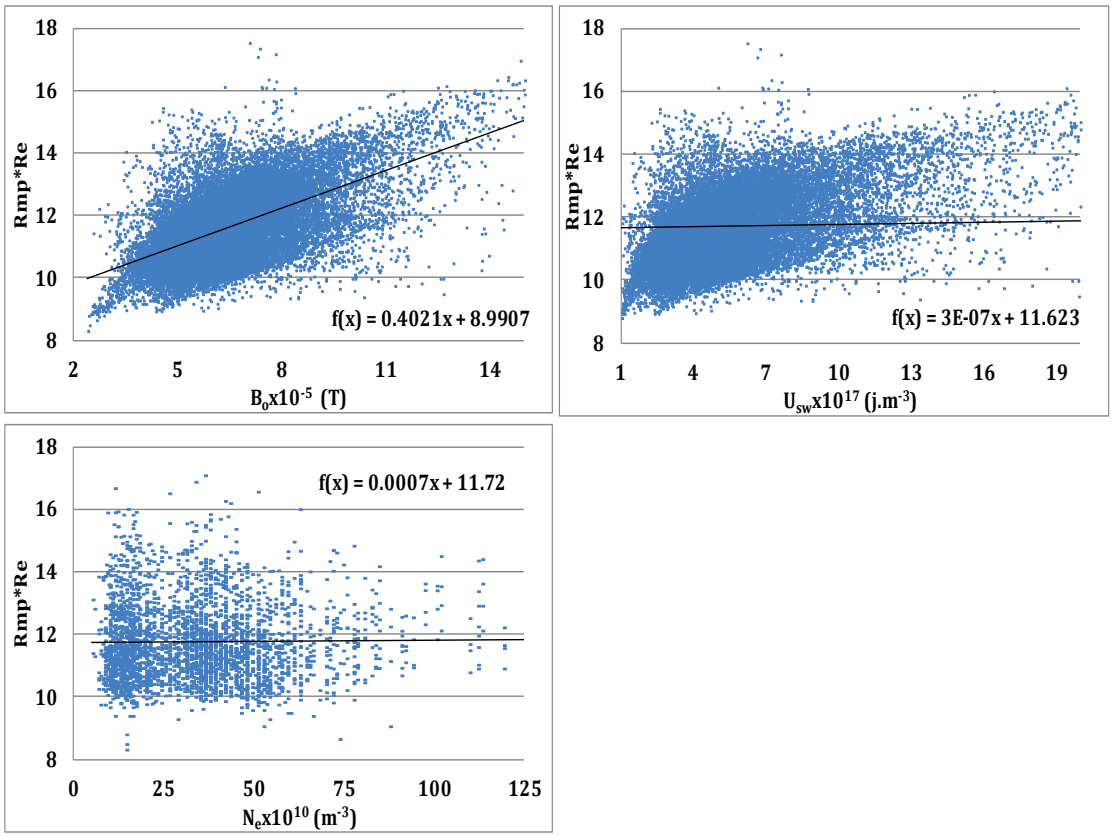

Fig.2: Hourly average of Earth's (R_{mp}) with (B_o), (U_{sw}) and (N_e) for years 2016- 2018.

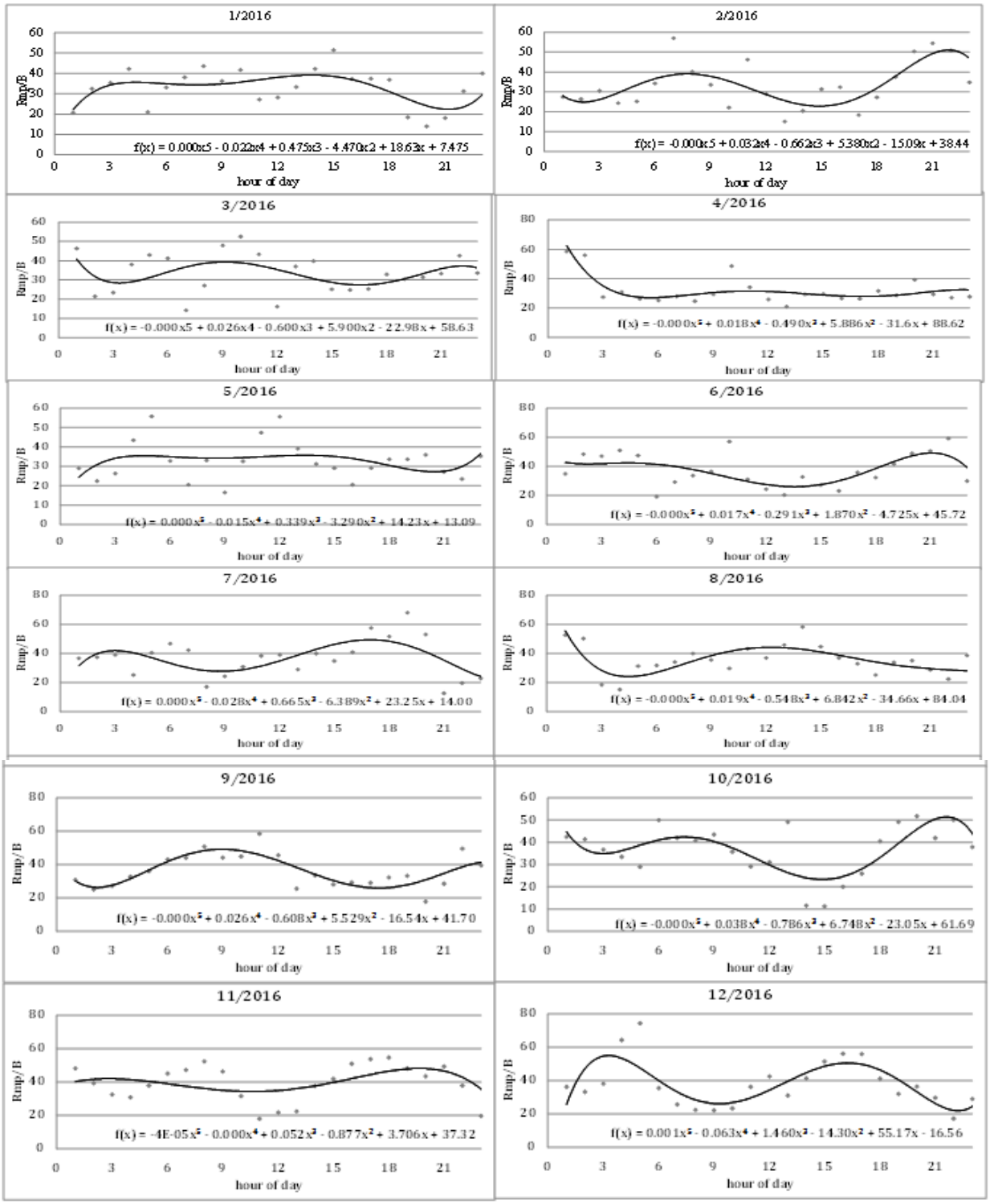

Fig. 3: Monthly median of (R_{mp}/B_o) for year 2016.

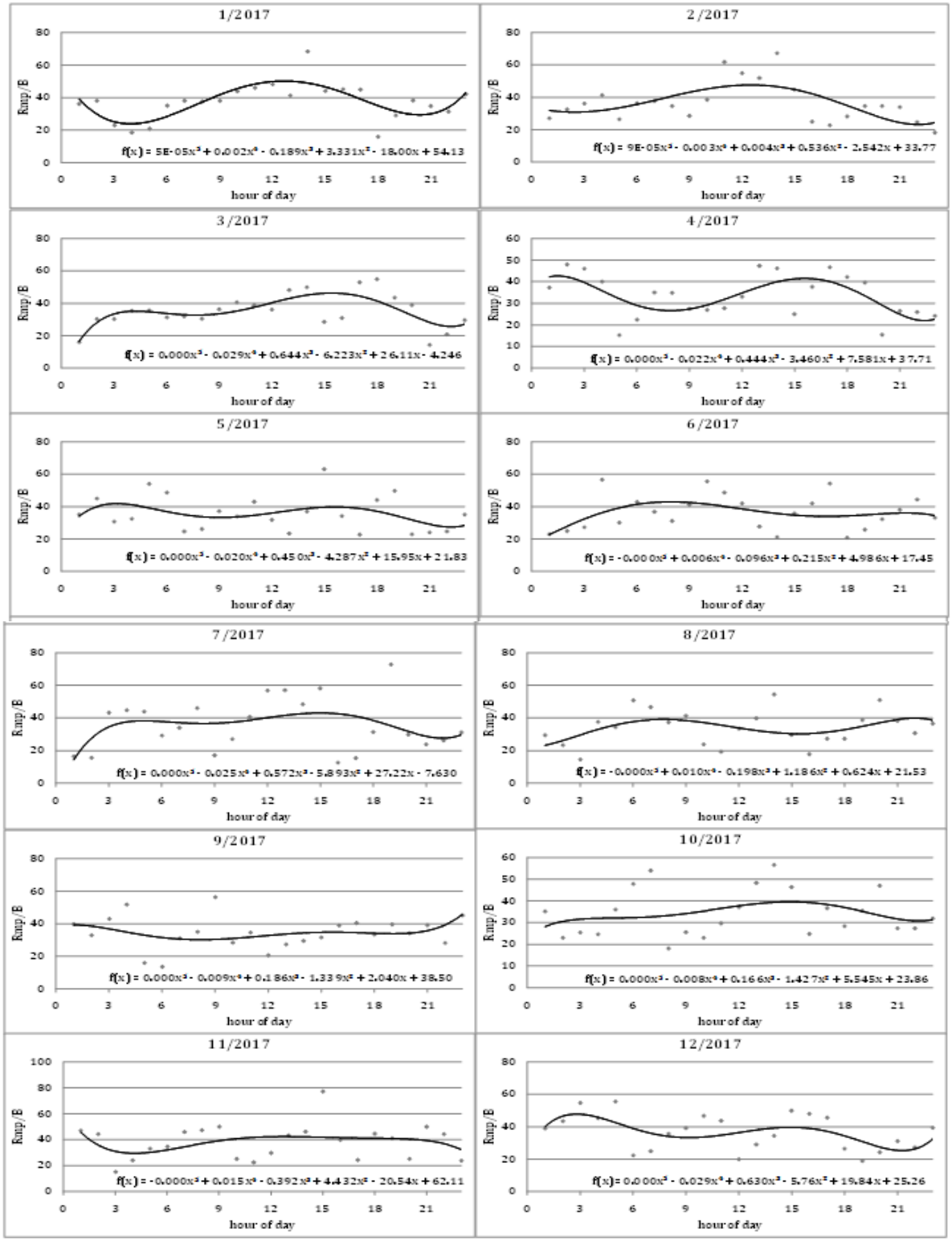

Fig. 4: Monthly median of (R_{mp} /B_o) for year 2017.

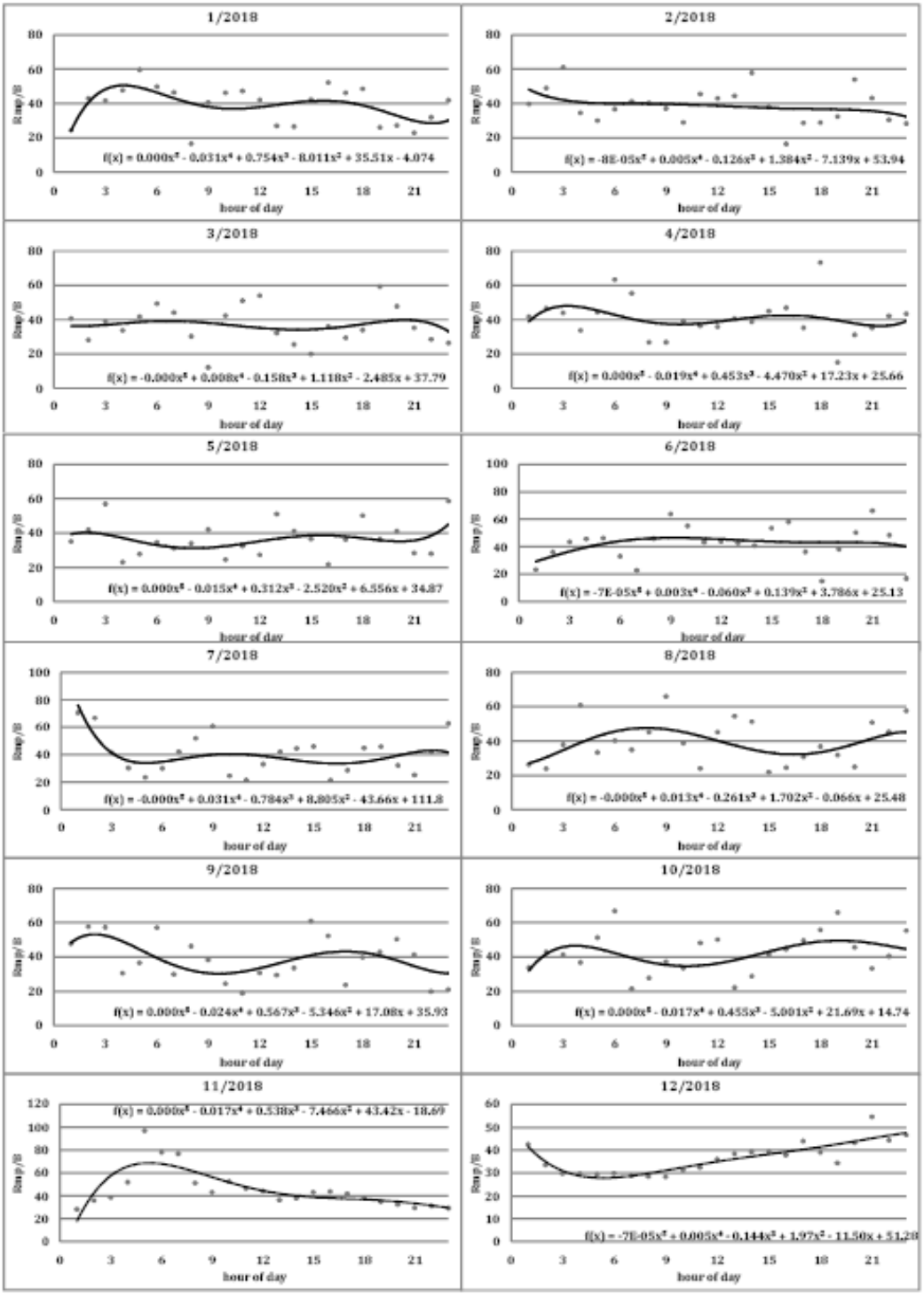

Fig. 5: Monthly median of (Rmp /Bo) for year 2018.

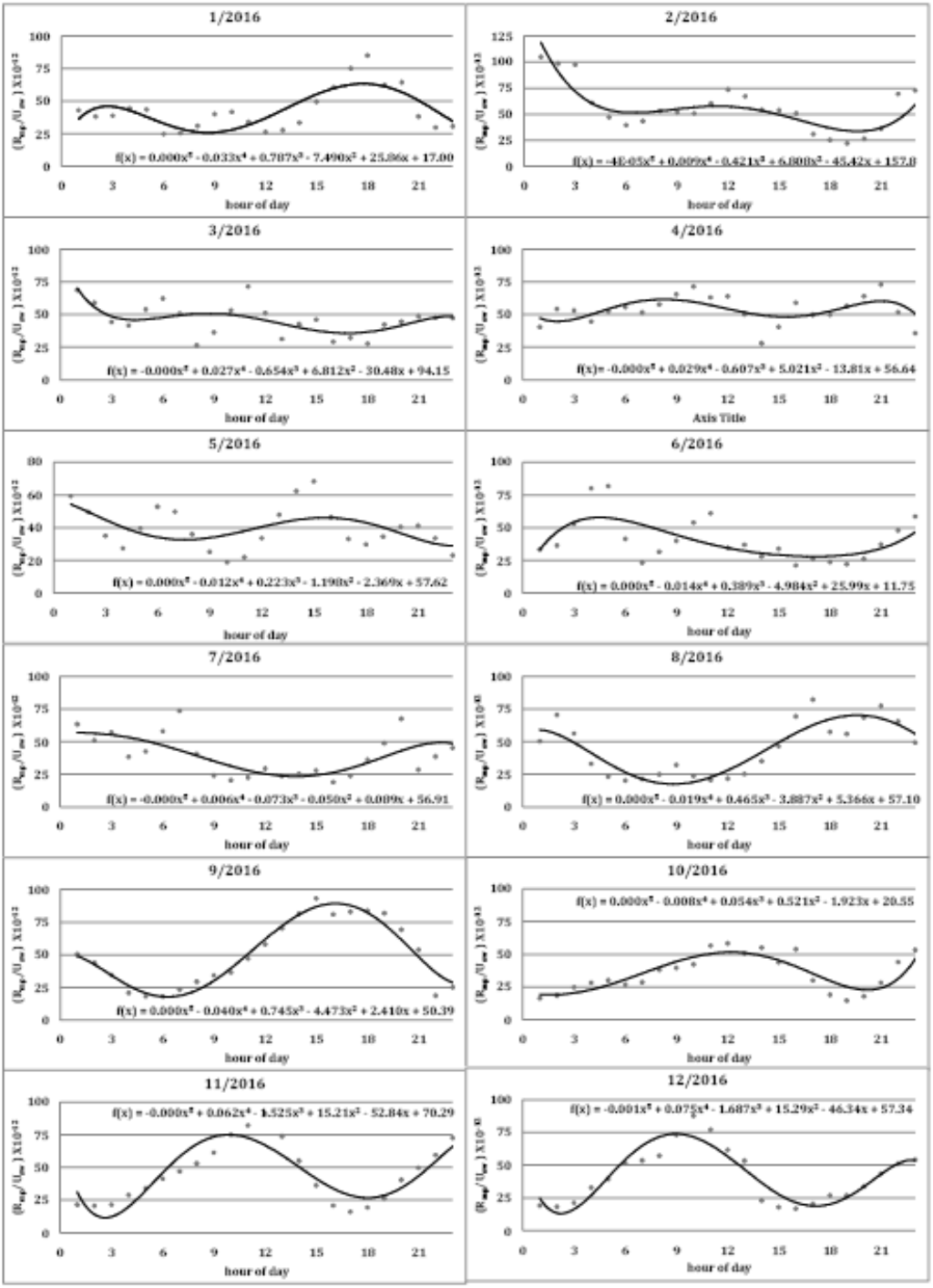

Fig. 6: Monthly median of (Rmp /Usw) for year 2016.

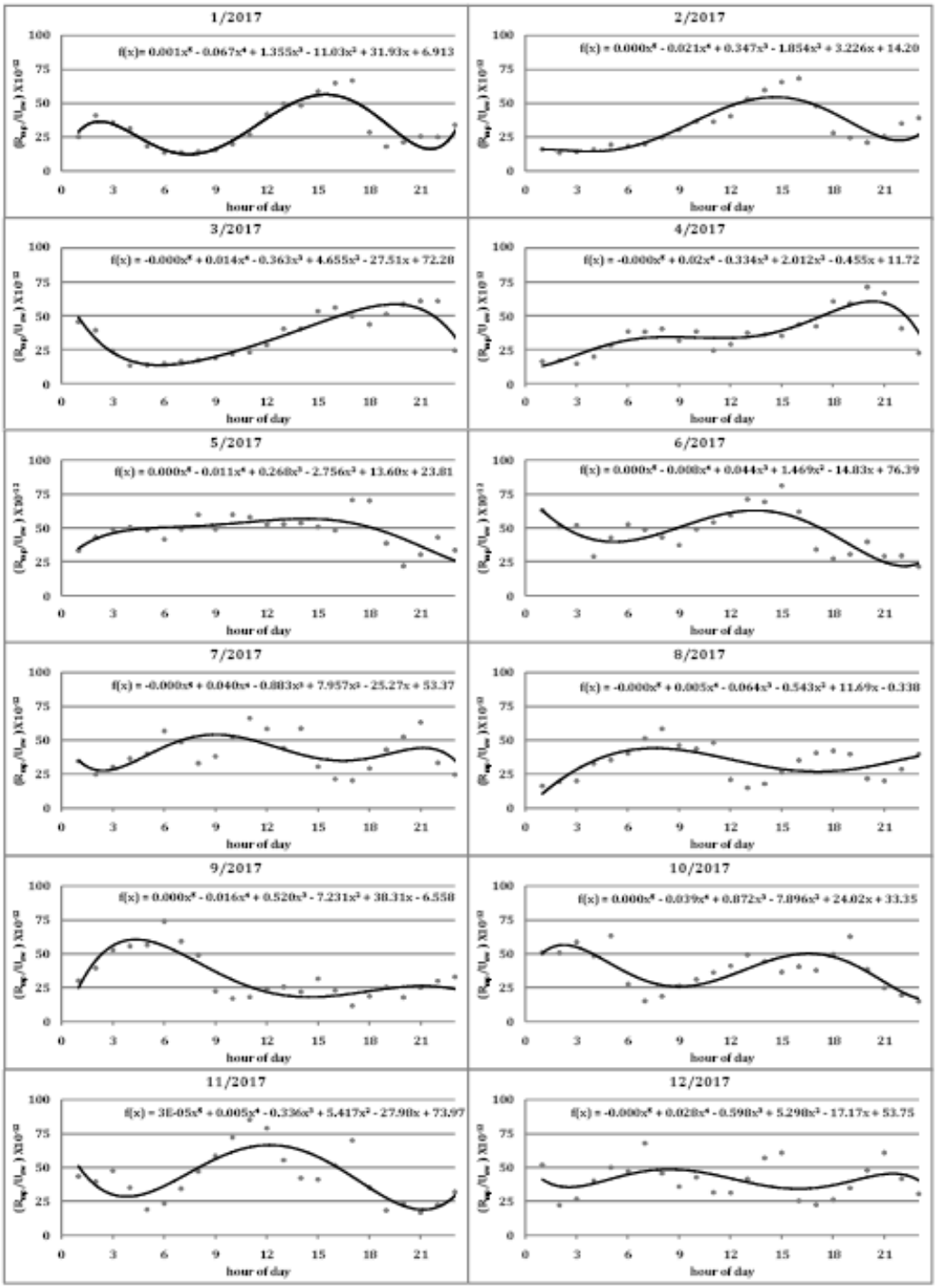

Fig. 7: Monthly median of (Rmp /Usw) for year 2017.

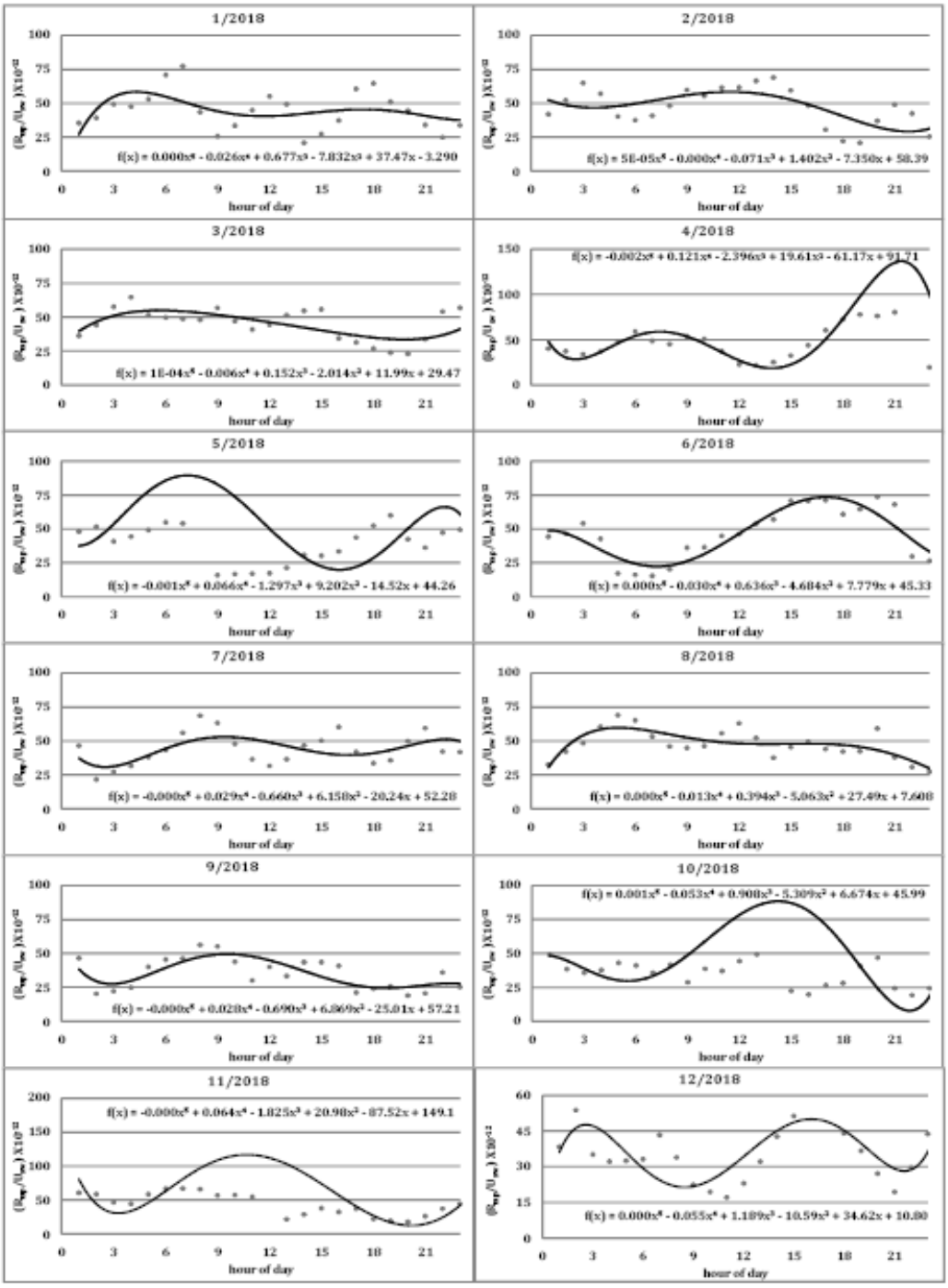

Fig. 8: Monthly median of (R_{mp} /U_{sw}) for year 2018.

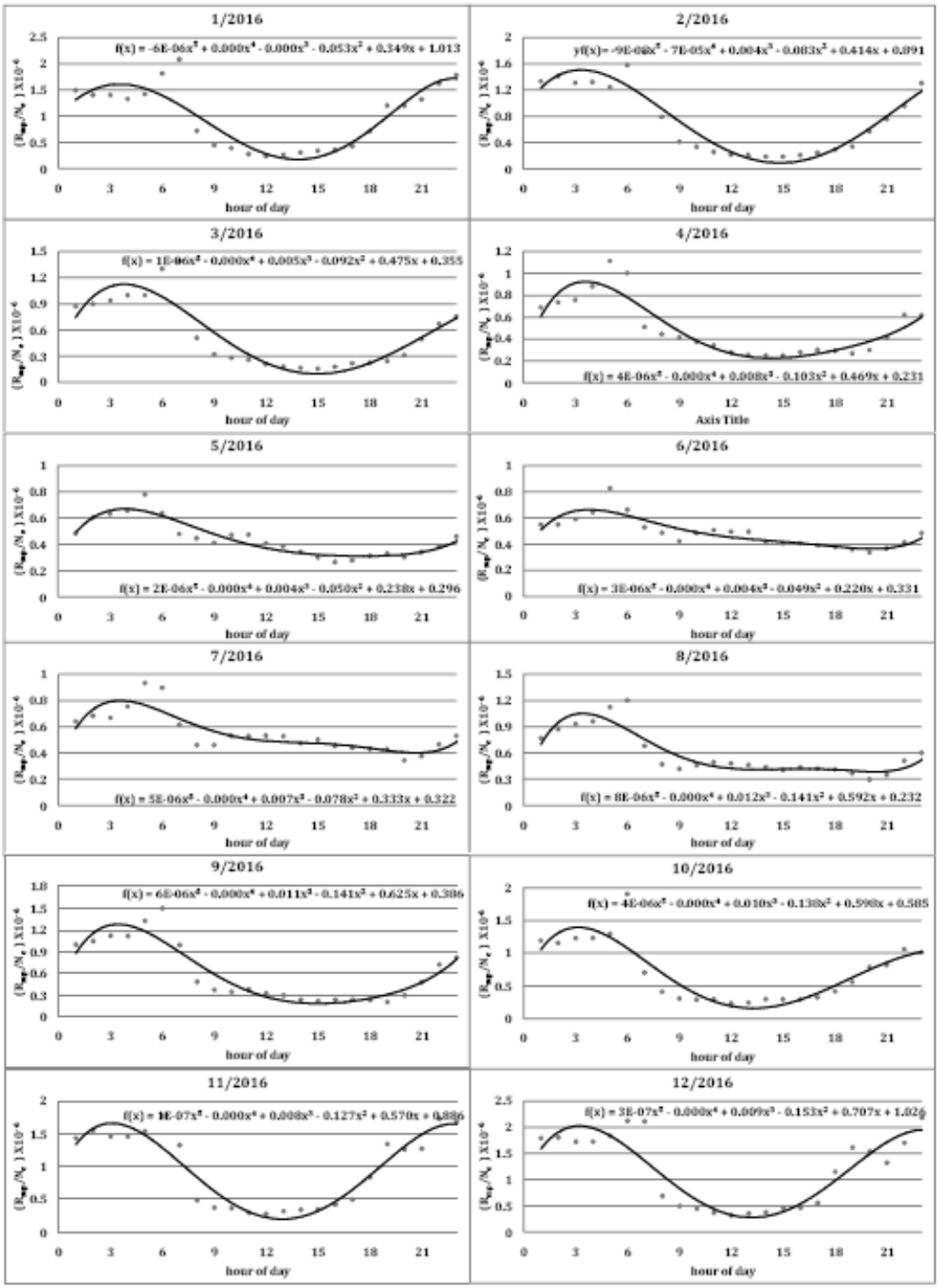

Fig. 9: Monthly median of (Rmp /Ne) for year 2016.

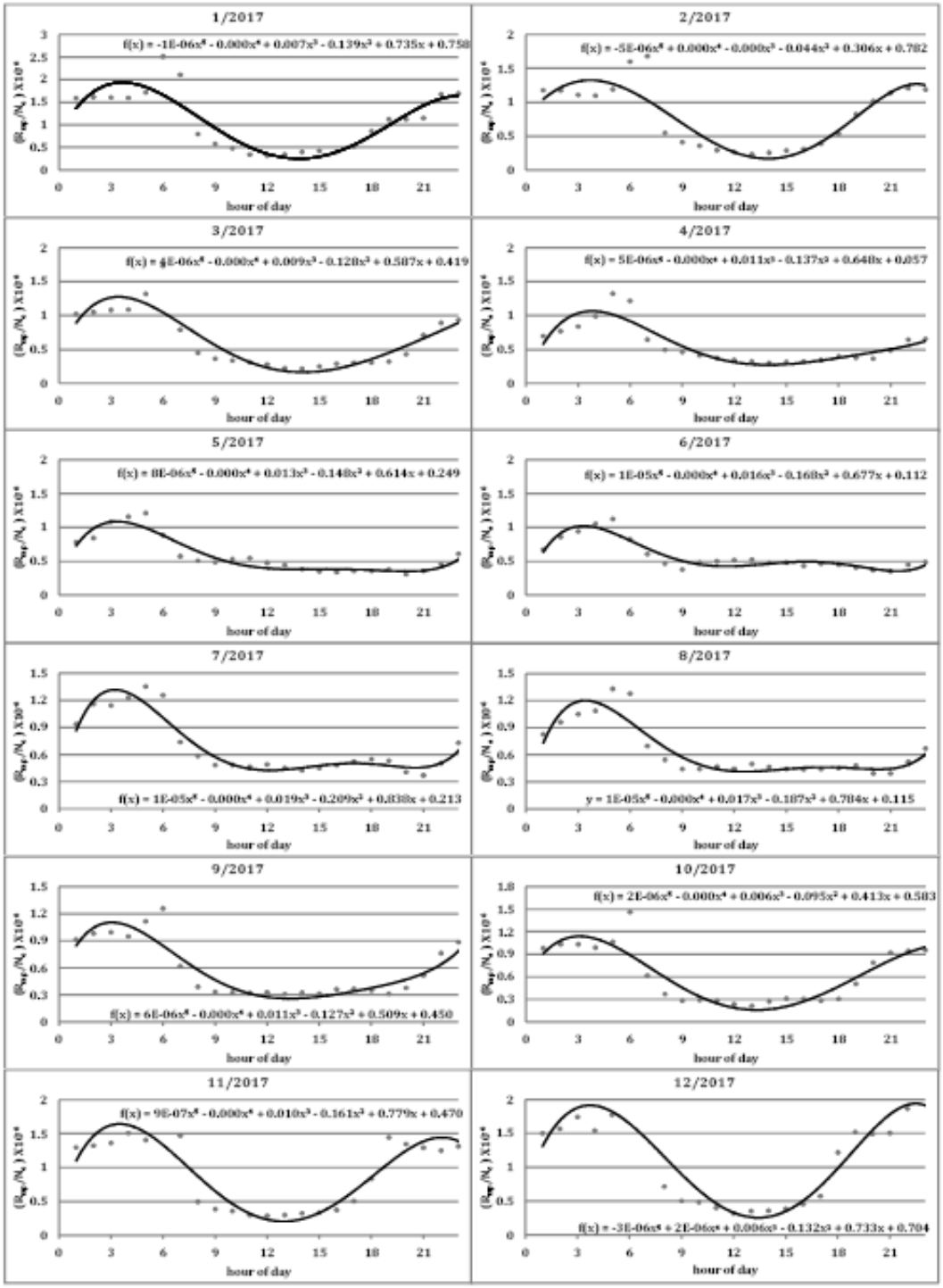

Fig. 10: Monthly median of (Rmp /Ne) for year 2017.

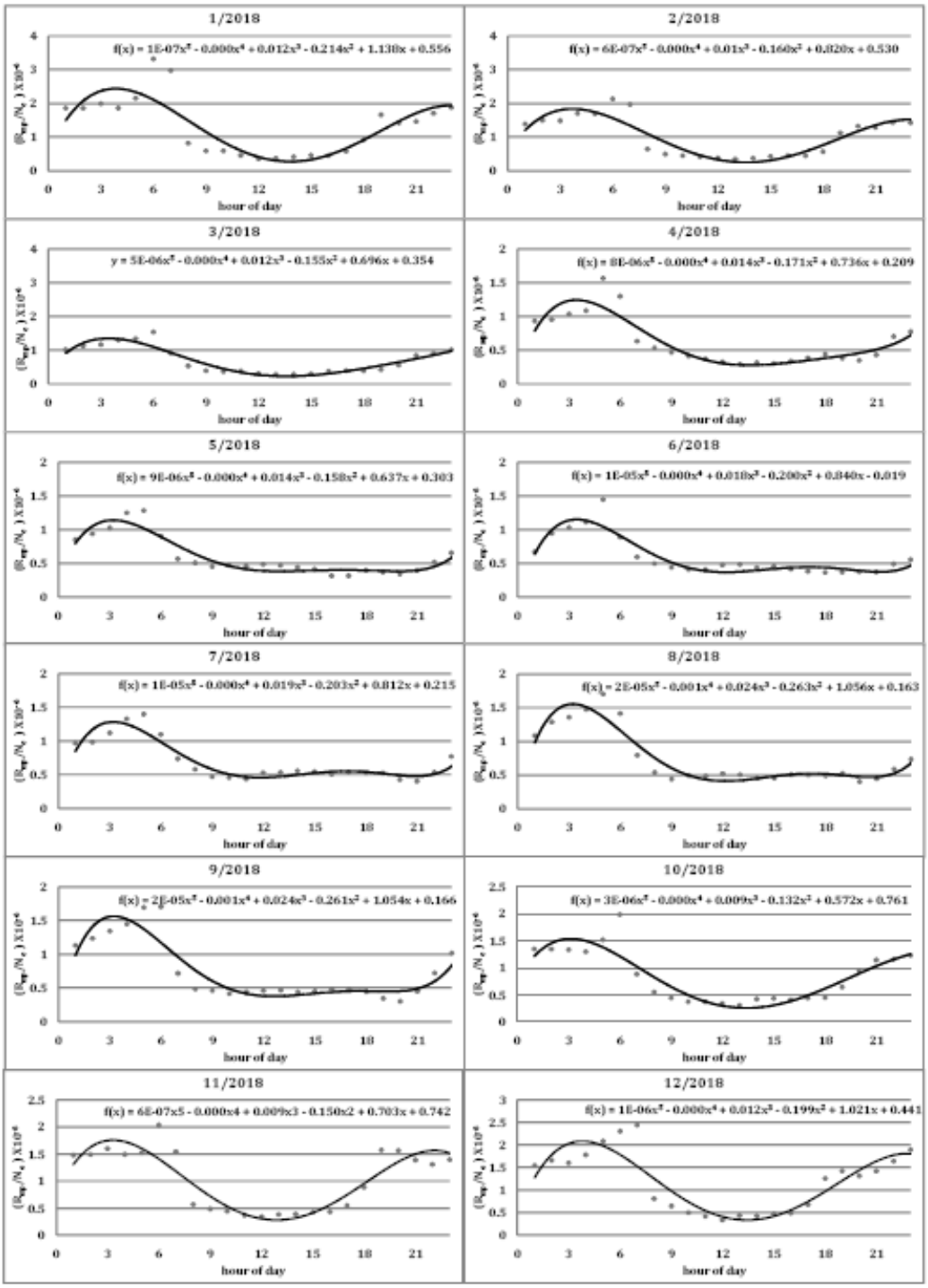

Fig. 11: Monthly median of (Rmp /Ne) for year 2018.

Table 2: Four coefficients of polynomial fitting equations for (R_{mp}/B_o) with days of year 2016.

Month	a_0	a_1	a_2	a_3
1	+ 7.475	+ 18.63	- 4.470	+ 0.475
2	+ 38.44	- 15.09	+ 5.380	- 0.662
3	+ 58.63	- 22.98	+ 5.900	- 0.60
4	+ 88.62	- 31.6	+ 5.886	- 0.490
5	+ 13.09	+ 14.23	- 3.290	+ 0.339
6	+ 45.72	- 4.725	+ 1.870	- 0.291
7	+ 14.00	+ 23.25	- 6.389	+ 0.665
8	+ 84.04	- 34.66	+ 6.842	- 0.548
9	+ 41.70	- 16.54	+ 5.529	- 0.608
10	+ 61.69	- 23.05	+ 6.748	- 0.786
11	+ 37.32	+ 3.706	- 0.877	+ 0.052
12	- 16.56	+ 55.17	- 14.30	+ 1.460

Table 3: Four coefficients of polynomial fitting equations for (R_{mp}/B_o) with days of year 2017.

Month	a_0	a_1	a_2	a_3
1	+ 54.13	- 18.00	+ 3.331	- 0.189
2	+ 33.77	- 2.542	+ 0.536	+ 0.004
3	- 4.246	+ 26.11	- 6.223	+ 0.644
4	+ 37.71	+ 7.581	- 3.460	+ 0.444
5	+ 21.83	+ 15.95	- 4.287	+ 0.450
6	+ 17.45	+ 4.986	+ 0.215	- 0.096
7	- 7.630	+ 27.22	- 5.893	+ 0.572
8	+ 21.53	+ 0.624	+ 1.186	- 0.198
9	+ 38.50	+ 2.040	- 1.339	+ 0.186
10	+ 23.86	+ 5.545	- 1.427	+ 0.166
11	+ 62.11	- 20.54	+ 4.432	- 0.392
12	+ 25.26	+ 19.84	- 5.76	+ 0.630

Table 4: Four coefficients of polynomial fitting equations for (R_{mp}/B_o) with days of year 2018.

Month	a_0	a_1	a_2	a_3
1	- 4.074	+ 35.51	- 8.011	+ 0.754
2	+ 53.94	- 7.139	+ 1.384	- 0.126
3	+ 37.79	- 2.485	+ 1.118	- 0.158
4	+ 25.66	+ 17.23	- 4.470	+ 0.453
5	+ 34.87	+ 6.556	- 2.520	+ 0.312
6	+ 25.13	+ 3.786	+ 0.139	- 0.060
7	+ 111.8	- 43.66	+ 8.805	- 0.784
8	+ 25.48	- 0.066	+ 1.702	- 0.261
9	+ 35.93	+ 17.08	- 5.346	+ 0.567
10	+ 14.74	+ 21.69	- 5.001	+ 0.455
11	- 18.69	+ 43.42	- 7.466	+ 0.538
12	+ 51.28	- 11.50	+ 1.97	- 0.144

Table 5: Four coefficients of polynomial fitting equations for (R_{mp}/U_{sw}) with days of year 2016.

Month	a_0	a_1	a_2	a_3
1	+ 17.00	+ 25.86	- 7.490	+ 0.787
2	+ 157.8	- 45.42	+ 6.808	- 0.421
3	+ 94.15	- 30.48	+ 6.812	- 0.654
4	+ 56.64	- 13.81	+ 5.021	- 0.607
5	+ 57.62	- 2.369	- 1.198	+ 0.223
6	+ 11.75	+ 25.99	- 4.984	+ 0.389
7	+ 56.91	+ 0.089	- 0.050	- 0.073
8	+ 57.10	+ 5.366	- 3.887	+ 0.465
9	+ 50.39	+ 2.410	- 4.473	+ 0.745
10	+ 20.55	- 1.923	+ 0.521	+ 0.054
11	+ 70.29	- 52.84	+ 15.21	- 1.525
12	+ 57.34	- 46.34	+ 15.29	- 1.687

Table 6: Four coefficients of polynomial fitting equations for (R_{mp}/U_{sw}) with days of year 2017.

Month	a_0	a_1	a_2	a_3
1	+ 6.913	+ 31.93	- 11.03	+ 1.355
2	+ 14.20	+ 3.226	- 1.854	+ 0.347
3	+ 72.28	- 27.51	+ 4.655	- 0.363
4	+ 11.72	- 0.455	+ 2.012	- 0.334
5	+ 23.81	+ 13.60	- 2.756	+ 0.268
6	+ 76.39	- 14.83	+ 1.469	+ 0.044
7	+ 53.37	- 25.27	+ 7.957	- 0.883
8	- 0.338	+ 11.69	- 0.543	- 0.064
9	- 6.558	+ 38.31	- 7.231	+ 0.520
10	+ 33.35	+ 24.02	- 7.896	+ 0.872
11	+ 73.97	- 27.98	+ 5.417	- 0.336
12	+ 53.75	- 17.17	+ 5.298	- 0.598

Table 7: Four coefficients of polynomial fitting equations for (R_{mp}/U_{sw}) with days of year 2018.

Month	a_0	a_1	a_2	a_3
1	- 3.290	+ 37.47	- 7.832	+ 0.677
2	+ 58.39	- 7.350	+ 1.402	- 0.071
3	+ 29.47	+ 11.99	- 2.014	+ 0.152
4	+ 91.71	- 61.17	+ 19.61	- 2.396
5	+ 44.26	- 14.52	+ 9.202	- 1.297
6	+ 45.33	+ 7.779	- 4.684	+ 0.636
7	+ 52.28	- 20.24	+ 6.158	- 0.660
8	+ 7.608	+ 27.49	- 5.063	+ 0.394
9	+ 57.21	- 25.01	+ 6.869	- 0.690
10	+ 45.99	+ 6.674	- 5.309	+ 0.908
11	+ 149.1	- 87.52	+ 20.98	- 1.825
12	+ 10.80	+ 34.62	- 10.59	+ 1.189

Table 8. Four coefficients of polynomial fitting equations for (R_{mp}/N_e) with days of year 2016.

Month	a_0	a_1	a_2	a_3
1	+ 1.013	+ 0.349	- 0.053	0
2	+ 0.891	+ 0.414	- 0.083	+ 0.004
3	+ 0.355	+ 0.475	- 0.092	+ 0.005
4	+ 0.231	+ 0.469	- 0.103	+ 0.008
5	+ 0.296	+ 0.238	- 0.050	+ 0.004
6	+ 0.331	+ 0.220	- 0.049	+ 0.004
7	+ 0.322	+ 0.333	- 0.078	+ 0.007
8	+ 0.232	+ 0.592	- 0.141	+ 0.012
9	+ 0.386	+ 0.625	- 0.141	+ 0.011
10	+ 0.585	+ 0.598	- 0.138	+ 0.010
11	+ 0.886	+ 0.570	- 0.127	+ 0.008
12	+ 1.026	+ 0.707	- 0.153	+ 0.009

Table 9: Four coefficients of polynomial fitting equations for (R_{mp}/N_e) with days of year 2017.

Month	a_0	a_1	a_2	a_3
1	+ 0.758	+ 0.735	- 0.139	+ 0.007
2	+ 0.782	+ 0.306	- 0.044	0
3	+ 0.419	+ 0.587	- 0.128	+ 0.009
4	+ 0.057	+ 0.648	- 0.137	+ 0.011
5	+ 0.249	+ 0.614	- 0.148	+ 0.013
6	+ 0.112	+ 0.677	- 0.168	+ 0.016
7	+ 0.213	+ 0.838	- 0.209	+ 0.019
8	+ 0.115	+ 0.784	- 0.187	+ 0.017
9	+ 0.450	+ 0.509	- 0.127	+ 0.011
10	+ 0.583	+ 0.413	- 0.095	+ 0.006
11	+ 0.470	+ 0.779	- 0.161	+ 0.010
12	+ 0.704	+ 0.733	- 0.132	+ 0.006

Table 10: Four coefficients of polynomial fitting equations for (R_{mp}/N_e) with days of year 2018.

Month	a_0	a_1	a_2	a_3
1	+ 0.556	+ 1.138	- 0.214	+ 0.012
2	+ 0.530	+ 0.820	- 0.160	+ 0.01
3	+ 0.354	+ 0.696	- 0.155	+ 0.012
4	+ 0.209	+ 0.736	- 0.171	+ 0.014
5	+ 0.303	+ 0.637	- 0.158	+ 0.014
6	- 0.019	+ 0.840	- 0.200	+ 0.018
7	+ 0.215	+ 0.812	- 0.203	+ 0.019
8	+ 0.163	+ 1.056	- 0.263	+ 0.024
9	+ 0.166	+ 1.054	- 0.261	+ 0.024
10	+ 0.761	+ 0.572	- 0.132	+ 0.009
11	+ 0.742	+ 0.703	- 0.150	+ 0.009
12	+ 0.441	+ 1.021	- 0.199	+ 0.012

References

[1] C.T. Russell, Reports on Progress in Physics, 56, 6 (1993) 687-732.
[2] O. Takahiro, Journal of the Communications Research Laboratory, 49, 3 (2002) 62-74.
[3] Haje Korth , Catherine L. Johnson, Lydia Philpott, Nikolai A. Tsyganenko, Brian J. Anderson, Geophysical Research letter, 44, 20 (2017) 10147-10154.
[4] Z. Nemecek, J. Safrankova, R. E. Lopez, S. Dusik, L. Nouzak, L. Prech, J. Simunek, J. H. Shue, Advances in Space Research, 58 (2016) 240-248.
[5] Michel Blanc, R. Kallenbach, N. V.Erkaev, Space Science Reviews, 116 (2005) 227-298.
[6] S. Baraka and L. Ben-Jaffel, J. of Geophysical Research, 112, A06212 (2007) 1-15.
[7] S. Baraka and L. Ben-Jaffel, Ann. Geophys., 29 (2011) 31-46.
[8] J. De Keyser, S. Stankov, T. Verhulst, 130, 2 (2014) 1-6.
[9] J.H. Shue, J.K. Chao, H.C. Fu, C.T. Russell, J. Geophys. Res., 102 (A5) (1997) 9497-9511.
[10] B.Muawad, Mohammed Yousef, Shahinaz Yousef, A.Walid, the 5th International Conference on Modern Trends in Physics Research WSP, 9914 (2016) 77-83.
[11] U.L. Kumar, Billin Susan Varghese, P. J. Kurian, Indian Journal of Radio & Space Physics, 46 (2017) 27-31.
[12] D.N. Baker, J. Erickson, J.F. Fennell, J.C. Foster, A.N. Jaynes1, P.T. Verronen, Space Sci Rev, 214, 17 (2017) 1-60.
[13] Reik V. Donner, Veronika Stolbova, Georgios Balasis, Jonathan F. Donges, Marina Georgiou, Stelios M. Potirakis, Jürgen Kurths, Physics.ao-ph, (2018) 1-23.
[14] G. V. Khazanov, R. M. Robinson, E. Zesta, D. G. Sibeck, M. Chu, G. A. Grubbs, Space Weather, 10 (2018) 1-9.